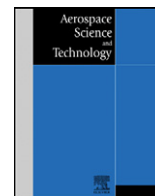




Contents lists available at ScienceDirect

## Aerospace Science and Technology

www.elsevier.com/locate/aescte



## An integrated approach for optimization of solid rocket motor

Ali Kamran\*, Liang Guozhu

School of Astronautics, Beijing University of Aeronautics and Astronautics (BUAA), 37 XueYuan Road, HaiDian District, Beijing, 100191, China

## ARTICLE INFO

## Article history:

Received 17 July 2010

Received in revised form 26 February 2011

Accepted 15 March 2011

Available online xxxx

## Keywords:

Solid rocket motor

Multidisciplinary design and optimization

Heuristics

CAD

## ABSTRACT

An integrated approach using hyper-heuristic based on meta-heuristics is applied in optimization of solid rocket motor. We propose a non-learning random function to control low-level meta-heuristics to increase certainty of global solution. A comprehensive empirical study investigates the performance of the proposed algorithm yielding satisfactory results. Design of solid rocket motor becomes an exigent task when accounting for chamber design, nozzle design, ballistic performance calculations as well as grain geometry and regression. CAD modeling overcomes the limitation posed by analytical expression thus increased model fidelity. CAD model allows different sub-systems to be modeled separately that not only prevents feature creation failures but also allows ease in modification of the model. Motor performance is calculated using a simplified ballistic model. Mass is the impetus driver on performance, and so considered as core of solid rocket motor design process. Therefore, we intend to minimize gross mass through hyper-heuristic approach. The approach produced satisfactory results for test case.

© 2011 Elsevier Masson SAS. All rights reserved.

## 1. Introduction

Solid rocket motor (SRM) design is a highly integrated process requiring synergistic compromise and tradeoffs of many parameters. The synthesis of an effective compromise requires balanced emphasis in sub-systems, unbiased tradeoffs, and evaluation of many alternatives. Multidisciplinary design optimization (MDO) is an emerging field in aerospace engineering that attempts to introduce a structured methodology to locate the best possible design in a multidisciplinary environment. In fact, MDO can be considered to be a discipline in and of itself with an intention of acting as an agent to bind the other disciplines together [34]. MDO methods can be either from the gradient based class of methods, non-gradient based methods, heuristics, parametric methods and so on. Each breed of methods has its strengths and weaknesses, and each is suitable for different types of problems [26]. In MDO the best choice of optimization method or combination of methods depends on the features of the given multidisciplinary problem. These include heterogeneous mixes of analysis codes, discrete design parameter values, non-differentiable functions, large number of design variables and a large number of design constraints. In addition, it is dependent on the organization of data communication and execution paths of various interconnected disciplines.

The subject of solid rocket motor design and optimization is quite vast. Its application varies from small igniters to the current heavy launch system like the space shuttle booster motor.

Many approaches, starting from gradient methods to basic heuristics, specially tailored meta-heuristics and hybrid heuristics have been used for design and optimization process of SRM system parameters and sub-components. Design and optimization of SRM have evolved with computing power; Refs. [2,3,5,6,15,22,24,27,31,33,36,38,39] portray the different modeling and optimization methods incorporated. A strong need arises to improve SRM modeling and the application of optimization technique. Present research effort proposes a solution strategy in trying to improve the design process considering both modeling and optimization issues.

SRM modeling is tedious if strictly dependent on analytical expressions for mass and volume calculation. Sub-assemblies connections can be particularly sensitive, and the modeling can be restricted to a certain range. CAD can prove to be of enormous potential. Present study uses a parametric approach to construct solid models of sub-systems thus providing a high degree of flexibility in the design process.

Increase in computational power has limited the use of conventional methods as they are dominated by reformatting, transforming, and translating of data between design disciplines and analysis modules. This will lead to inferior solution. Meta-heuristics proved their superiority over conventional methods but cannot adopt universal settings for different design scenarios. The No Free Lunch Theorem [41] ended the supremacy of individual heuristics. Present-day demand of variable scale design necessitates the need of algorithms independent of the solution domain. Hyper-heuristic approach (HHA) seems to be the way forward.

The approach presented in this study uses a non-learning stochastic function applied to low-level meta-heuristics. Genetic

\* Corresponding author. Tel.: +86 13693569259.

E-mail address: a1k1s1@hotmail.com (A. Kamran).

## Nomenclature

$A$	Area at any location along nozzle length.....	$\text{mm}^2$	$r_n$	Mean radius of curvature	
$A_{bk}$	Burning area at $k$ th step.....	$\text{mm}^2$	$T_L$	Temperature of charred layer.....	K
$A_t$	Throat area.....	$\text{mm}^2$	$T_o, T_g$	Gas temperature.....	K
$a$	Burn rate coefficient.....	$\text{mm/s/Pa}^n$	$T_a$	Ablation temperature.....	K
$a'$	Thermal diffusivity.....	$\text{m}^2/\text{s}$	$T_i$	Initial temperature.....	K
$a_1$	Thermal diffusivity of virgin material.....	$\text{m}^2/\text{s}$	$T_w$	Nozzle wall temperature.....	K
$a_2$	Thermal diffusivity of charred material.....	$\text{m}^2/\text{s}$	$T^*$	Permissible casing wall temperature.....	K
$C_F$	Thrust coefficient		$t, t_b$	Burning time.....	s
$C_p$	Specific heat at constant pressure.....	J/kg K	$t_a$	Ablation thickness.....	mm
$c^*$	Characteristic velocity.....	m/s	$t_c$	Carbonization thickness.....	mm
$D$	Chamber diameter.....	mm	$t_{tot}$	Total thickness.....	mm
$d_e$	Exit diameter.....	mm	$V_a$	Ablation rate.....	$\text{mm/s}$
$d_t$	Throat diameter.....	mm	$V_{case}$	Propellant volume.....	$\text{m}^3$
EPDM	Ethylene propylene diene monomer		$V_k$	Grain volume at $k$ th step.....	$\text{m}^3$
$F$	Thrust.....	kN	$V_p$	Propellant volume.....	$\text{m}^3$
$f_{os}$	Factor of safety		$w_k$	Web at $k$ th step	
HTPB	Hydroxy terminated polybutadine		$X$	Insulation thickness.....	mm
$H_{eff}$	Effective heat of ablation.....	J/kg	$XT$	Thickness of charred layer.....	mm
$I$	Total impulse.....	kN s	$x$	Axial location along nozzle length.....	mm
$I_{sp}$	Specific impulse.....	s	$y$	Radius at any axial location along nozzle length.....	mm
$k$	Burning step		$\alpha$	Convergent half angle.....	deg
$L$	Length of motor.....	mm	$\alpha_t$	Convective heat transfer coefficient.....	$\text{W/m}^2\text{K}$
$M_a$	Mach number at each location along nozzle length		$\beta$	Divergent half angle.....	deg
$M_C$	Mass of casing.....	kg	$\gamma$	Specific heat constant	
$M_N$	Mass of nozzle.....	kg	$\rho_p$	Propellant density.....	$\text{kg/m}^3$
$M_i$	Mass of insulation and liner.....	kg	$\rho$	Density.....	$\text{kg/m}^3$
$m_p$	Mass of propellant		$\eta_{vol}$	Volumetric efficiency	
$n$	Pressure exponent		$\xi$	Weld coefficient	
$p_{amb}$	Ambient pressure.....	bar	$\delta_{cy}$	Thickness of casing.....	mm
$p_c$	Chamber pressure.....	bar	$\sigma$	Material strength.....	MPa
$p_e$	Nozzle exit pressure.....	bar	$\lambda_1$	Thermal conductivity of virgin material.....	$\text{W/mK}$
$P_{max}$	Maximum pressure.....	bar	$\mu$	Kinematic viscosity.....	$\text{kg/m s}$
$P_r$	Prandtl number		$\varepsilon$	Nozzle area ratio	
$\rho_1$	Density of charred layer.....	$\text{kg/m}^3$	$\Psi$	Length to diameter ratio of grain	

algorithm (GA), particle swarm optimization (PSO) and simulated annealing (SA) are the selected low-level meta-heuristics. The primary purpose is to avoid local minima and not selection of appropriate meta-heuristics. The intention is not to reduce the computational time, selection of heuristic but to improve solution quality. The proposed methodology attains the defined objective by providing diversity to population and altering search direction by injecting feasible solutions. This, however, may lead to additional computational time but at the same will serve as a tool to avoid local minima. The goal is not necessarily to 'beat' previously employed methods but to obtain satisfactory results by employing a generalized method that can 'solve' different problem scenarios with no or limited tuning of the algorithm.

This manuscript is organized in three parts. First section explains design problem of SRM. Sub-systems of chamber, nozzle, grain (geometry and regression) and ballistic analysis are given in this section. Second section covers hyper-heuristic approach. Last section covers SRM design problem formulation, results, and conclusions.

## 2. Solid rocket motor design

Solid rocket motor comprises of a combustion chamber, nozzle, and grain. Design variables of these sub-systems are connected to system level variables. A strong interaction exists between the different disciplines therefore SRM design is an integrated process requiring synergistic compromise and tradeoffs of many param-

eters. The synthesis of an effective compromise requires balanced emphasis in sub-systems, unbiased tradeoffs, and the evaluation of many alternatives. Fig. 1 outlines the SRM design analysis approach. Solid line shows the optimization of system level parameters once the convergence criteria is met, grain design optimization is shown with dotted line. The intricacy of affects of sub-systems on each other makes the design mechanism of SRM significantly hard. The interaction of sub-systems is explained in design structure matrix (Fig. 2). SRM sizing, mass and volume require adequate definitions of attachment collars. The basic sizing parameters will drive the CAD model, perhaps with an empirical relation between collar faces and thickness for igniter/nozzle/payload/tail skirt. The relations shown in detail modeling of SRM simplify and improve design process from practical engineering point of view (Figs. 3–12). Detail design analysis devoted to combustion chamber, nozzle and grain is given below.

### 2.1. Combustion chamber

Vehicle requirement such as performance characteristics, envelope constraints, and mission profile govern the combustion chamber design. Motor case design leads to the selection of structural material and configuration achieving optimum performance while satisfying constraints. A thermal barrier is provided on the inner surface to prevent high temperature gases to have direct contact with metal. In the present work combustion chamber considered is a steel casing, lined with EPDM insulation. The casing comprises of

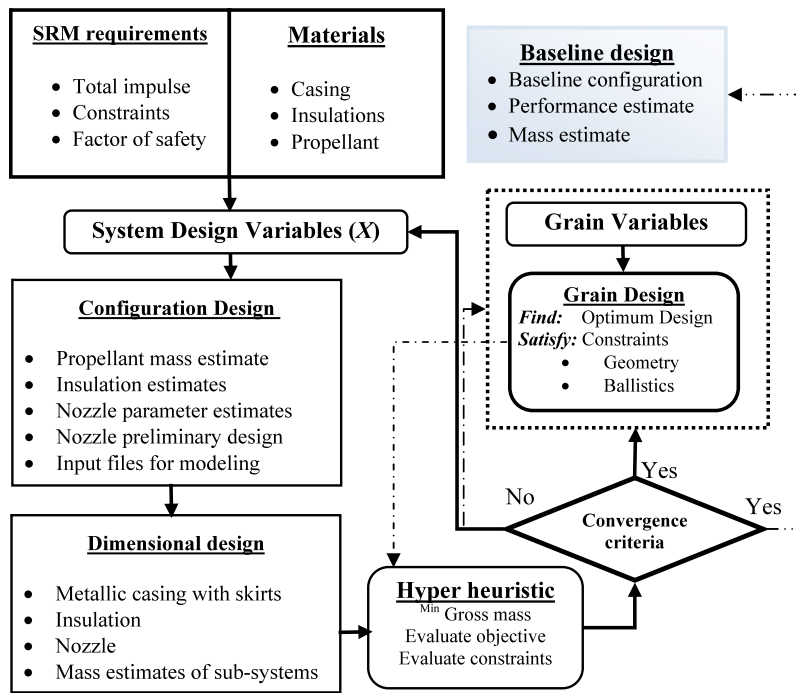


Fig. 1. SRM system design analysis.

<b>SRM Envelope</b>		Propellant mass,		Nozzle exit diameter
	<b>Grain</b>	Length, Diameter	Burn time, thrust	Total impulse
Overall dimensions of SRM	Insulation mass	<b>Chamber</b>	Inert mass	
Convergent angle Divergent angle	Insulation thickness		<b>Nozzle</b>	Area ratio
		Pressure	Burn time	<b>Ballistics</b>

Fig. 2. Coupling of design variables.

a cylindrical steel shell with domes on both ends. Forward and rear skirts are for attachment purposes. Front and rear collars are for igniter and nozzle attachments respectively. Fig. 3 shows detailed model of the metal casing. Chamber minimum wall thickness is calculated as:

$$\delta_{cy} = \frac{P_{max} D}{2\xi\sigma} f_{os} \quad (1)$$

To account for dome stresses a factor of safety of 1.4, weld coefficient of 0.98 and  $P_{max}$  of 1.2  $p_c$  are considered. The insulation layer ensures that the case will not be overheated. Generally, the cables for electronic modules run along casing length therefore during the working time of motor the case wall temperature should not exceed the permissible wall temperature of  $\sim 30^\circ\text{C}$ . The insulation thickness can be determined using formula [40]:

$$\frac{T^* - T_i}{T_L - T_i} = \frac{\text{erfc}\left(\frac{X T^*}{2\sqrt{a_2 t}}\right)}{\text{erfc}\left(\frac{X_L}{2\sqrt{a_2 t}}\right)}$$

$$\frac{T^* - T_i}{T_L - T_i} = \frac{\text{erfc}\left(\frac{X T^*}{2\sqrt{a_2 t}}\right)}{\text{erfc}\left(\frac{C_o}{\sqrt{a_2}}\right)} \quad (2)$$

where  $X_L = C_o \sqrt{t}$

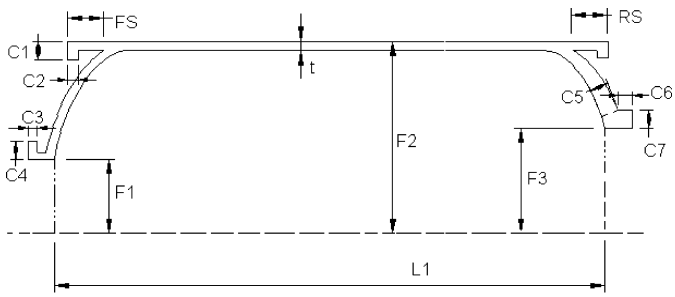
$$C_o = \left\{ \frac{2\lambda_1(T_o - T_L)}{p_1 X} \right\}^{1/2} \quad (3)$$

Grain burning regression dictates the insulation profile (Fig. 4). Liner mass is calculated with insulation mass with the thickness of 1 mm as they have almost same density.

## 2.2. Nozzle

The present study considers conical nozzle because of its simplicity. Designed nozzle is modeling via CAD to calculate the mass of the nozzle; compromise is made between thrust coefficient and mass of the nozzle to reach at optimum nozzle. Figs. 5 and 6 present nozzle geometry and contour respectively.

The thermal design of the nozzle is to maintain nozzle aerodynamic design insofar as is practical and to limit the temperature



- Chamber length, L1
- Chamber radius, F2
- Chamber thickness,  $t = \delta_{cy}$
- Front end opening, F1=0.1F2
- Rear end opening, F3=0.7F2
- Front collar width, C4=4t
- Front collar thickness, C3=3t
- (Front and rear end skirt length are same, FS=RS)
- Front skirt thickness, C2=2t
- Front skirt length, FS=50+12t
- Rear end thickness, C5=2t
- Rear end collar thickness, C6=22+2t
- Rear end collar width, C7=22+2t
- Rear end skirt length, RS=50+12t
- Front skirt width, C1=2t

Fig. 3. Cross section of chamber case.

of the structure to acceptable levels. A thermal liner forms the nozzle aerodynamic contour. An insulator is a material placed behind a liner to serve as a thermal barrier to protect the structural member from excessive temperature; a single material thickness often serves as both liner and insulator. 1D flow analysis along with heat transfer model calculates various insulation thicknesses. The convective heat transfer coefficient ( $\alpha_t$ ) is calculated by the well-known Bartz equation as under:

$$\alpha_t = \frac{b}{d_t^{0.2}} \left( \frac{\mu^{0.2} C_p}{P_r^{0.6}} \right)_{T_g^*} \left( \frac{p_c}{c^*} \right)^{0.8} \left( \frac{d_t}{r_n} \right)^{0.1} \left( \frac{A_t}{A} \right)^{0.9} \omega \quad (4)$$

$$\omega = \frac{1}{\left[ \frac{1}{2} \times \frac{T_w}{T_g^*} \left( 1 + \frac{\gamma-1}{2} M_a^2 \right) + \frac{1}{2} \right]^{0.68} \left[ 1 + \frac{\gamma+1}{2} M_a^2 \right]^{0.12}} \quad (5)$$

where

$$b = \begin{cases} 0.0245 & \text{in convergent section} \\ 0.026 & \text{in throat section} \\ 0.023 & \text{in divergent section} \end{cases}$$

Mach number along nozzle length is calculated as

$$\frac{A_y}{A_x} = \varepsilon = \frac{M_x}{M_y} \sqrt{\frac{\left\{ 1 + \left[ \frac{\gamma-1}{2} \right] M_y \right\}^{\frac{\gamma+1}{\gamma-1}}}{1 + \left[ \frac{\gamma-1}{2} \right] M_x}} \quad (6)$$

Ablation rate with respect to time can be given as:

$$t_{ab} = \frac{a^t}{V_a^2} \quad (7)$$

$$V_a = \frac{\sigma_t (T_0 - T_a)}{\rho H_{ref}} \quad (8)$$

$$t_a = V_a \left( \frac{t_b - a^t}{V_a^2} \right) \quad (9)$$

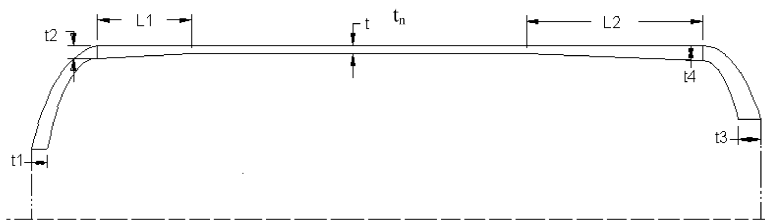
Also the carbonization thickness is given by the formula

$$t_c = \frac{2a^t}{V_a} \quad (10)$$

Thus the total thickness with a factor of safety is given by following equation:

$$t_{tot} = 1.2 \approx 1.5(t_a - t_c) \quad (11)$$

Figs. 5–12 present detailed description of models. Metallic portion of nozzle comprises of convergent part and a divergent support ring (Figs. 11, 12).



- Front taper length, L1 =0.2F2
- Rear taper length, L2=1.8F2
- Nominal thickness, t<sub>n</sub>
- Front start thickness, t1
- Rear start thickness, t3
- Front end thickness, t2=0.8t1
- Rear end thickness, t4=0.8t3

Fig. 4. Insulation profile.

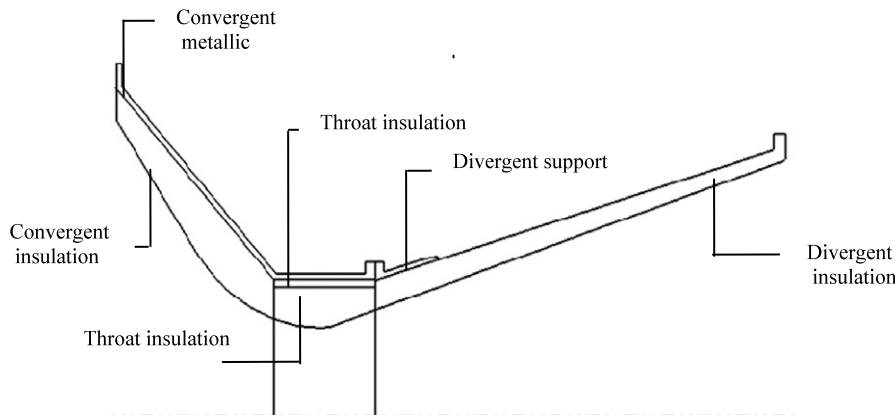


Fig. 5. Nozzle architecture.

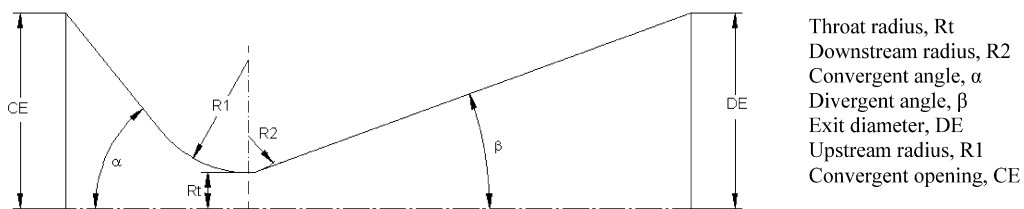


Fig. 6. Nozzle profile.

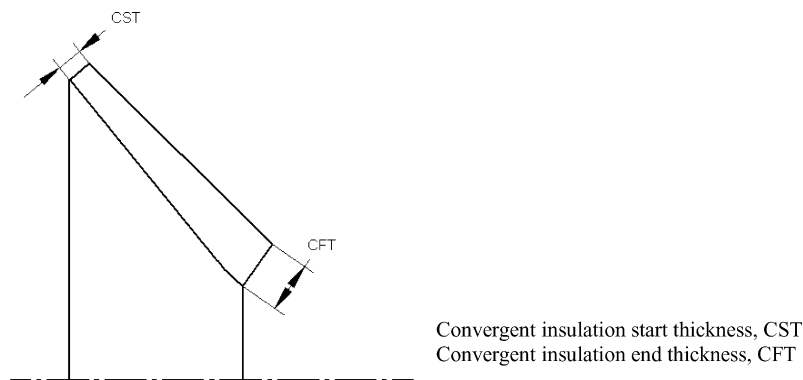


Fig. 7. Nozzle convergent section.

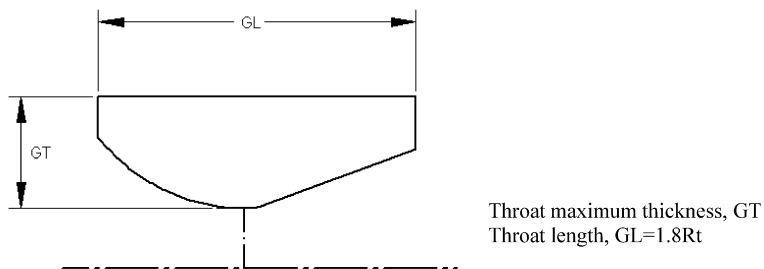


Fig. 8. Nozzle throat section.

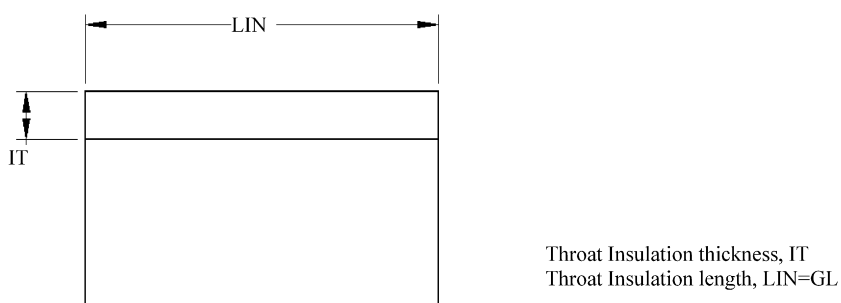


Fig. 9. Nozzle throat insulation.

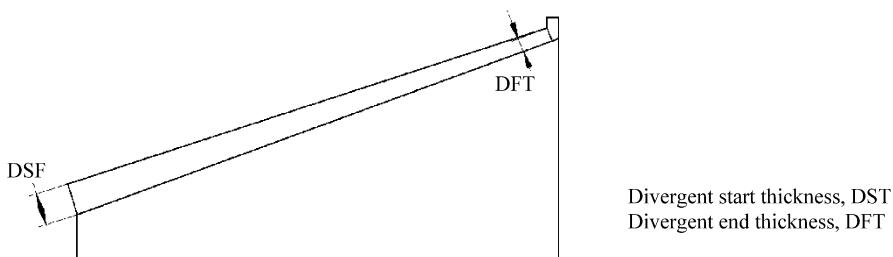
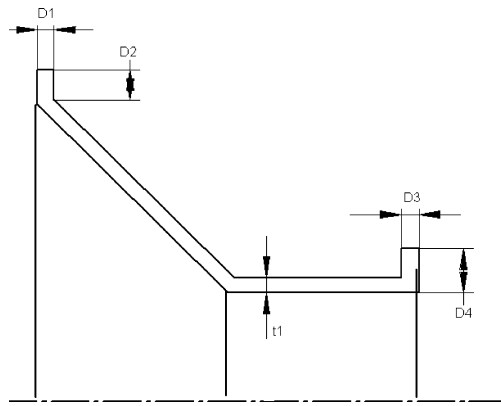
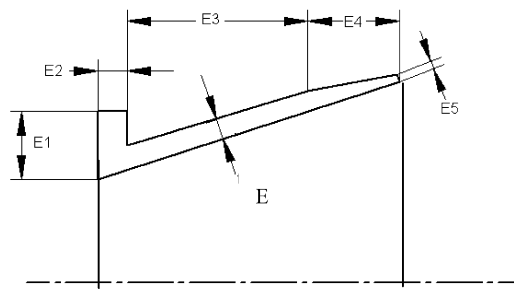


Fig. 10. Nozzle divergent section.



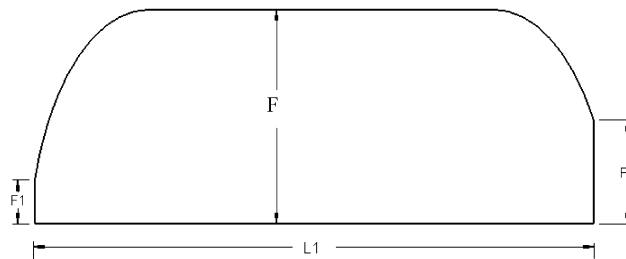
Convergent front collar thickness,  $D1=1.2t1$   
 Convergent front collar width,  $D2=4t1$   
 Convergent thickness,  $t1=1.3t$   
 Convergent rear collar thickness,  $D3=2t1$   
 Convergent rear collar width,  $D4=3t1$

Fig. 11. Nozzle convergent metallic section.



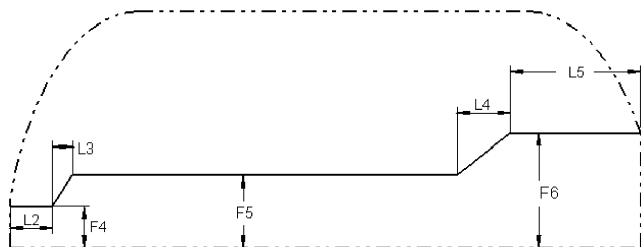
Divergent support collar width,  $E1=D4$   
 Divergent support collar thickness,  $E2$   
 Divergent support length,  $E3=2Rt$   
 Divergent support tapered length,  $Rt$   
 Tapered end thickness,  $E5=0.5t1$   
 Divergent support thickness,  $E=t1$

Fig. 12. Nozzle divergent metallic support.



Chamber length,  $L1$   
 Grain radius,  $F=F2-t-t_n$   
 Front end opening,  $F1$   
 Rear end opening,  $F3$

Fig. 13. Grain boundary.



Front web,  $L2$   
 Front end opening,  $F4$   
 Front cone,  $L3$   
 Core diameter,  $F5$   
 Rear cone,  $L4$   
 Rear cylinder length,  $L5$   
 Rear cylinder diameter,  $F6$

Fig. 14. Grain bore.

2.3. Grain

Grain design is most imperative in completing the design of any solid rocket motor. The essence is to evolve the burning surface and establish a relation between web burnt and the burning surface. The grain design and burning surface evolution of a complex 3D solid rocket propellant grain are modeled by CAD software using parametric modeling: subsequent propellant surface regression is simulated using offset feature. Present study considers Finocyl

grain configuration for the test case. The Finocyl (Fin in Cylinder) is a 3D internal burning grain configuration with relatively long duration and high thrust. It can provide a variety of thrust time trace depending on mission requirements. Grain is modeled in parts to provide ease and ensure lesser chances of surface creation failure.

Figs. 13–16 provide a detailed description of the grain modeling. Following steps explain the construction of grain configuration:

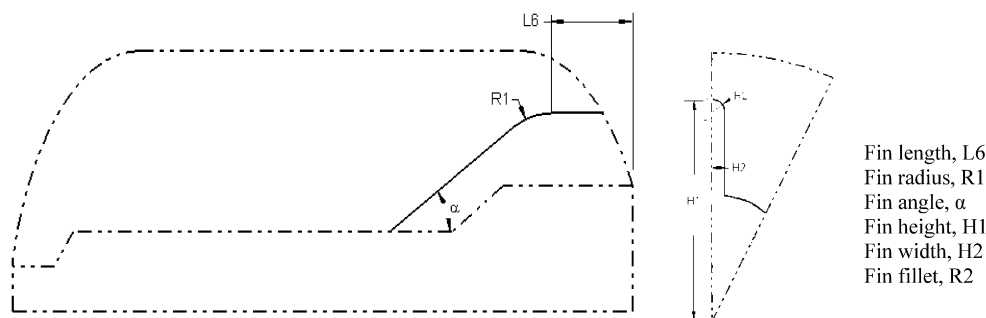


Fig. 15. Fin shape.

- Grain boundary is solid and constructed by revolve protrusion with no burning surface (Fig. 13).
- Grain bore is constructed by revolve surface and all surfaces burning (Fig. 14).
- Sharp corners are filleted to account for new surfaces that are created during burning (Fig. 16). Lines AB and BC are connected using CAD function "CONNECT", so that they remain connected during offsetting operation. Lines BC and CD are connected through a small fillet of radius 0.1 mm in the initial geometry. During offsetting the fillet radius is incremented by a value equal to web increment.
- Boolean function is used to subtract the solid within grain bore.
- Similar operation is performed for fins cross-section and axial shape with all surfaces burning (Fig. 15).
- Surface offset function available in CAD software is used to simulate burning, by offsetting the surface by a web increment equal and orthogonal in all direction.
- Boolean function is used at each web increment to subtract the solid within grain bore and fins to calculate new volume.
- Offsetting and Boolean operations are repeated till web is completely burnt.

The grain regression is achieved by a web increment equal in all direction; at each step new grain geometry is created automatically thereafter geometrical properties are estimated. Burning surface area is calculated as

$$A_{bk} = \frac{V_{k+1} - V_k}{w_{k+1} - w_k} \quad (12)$$

#### 2.4. Ballistic analysis

The chamber pressure is assumed to be uniform throughout the motor chamber; therefore, the burning rate is uniform as well. Steady state pressure is calculated by equating mass generated in the chamber to mass ejected through nozzle throat [4,10,35]. Following relation calculates the chamber pressure:

$$p_c = (\rho_p a c^* K)^{1/(1-n)} \quad (13)$$

where  $K = A_b/A_t$ , and thrust is calculated as

$$F = C_F p_c A_t \quad (14)$$

Thrust coefficient and total impulse is given as:

$$C_F = \sqrt{\frac{2\gamma^2}{\gamma-1} \left(\frac{2}{\gamma+1}\right)^{(\gamma+1)/(\gamma-1)} \left[1 - \left(\frac{p_e}{p_c}\right)^{(\gamma-1)/\gamma}\right]} + \frac{p_e - p_{amb}}{p_c} \epsilon \quad (15)$$

$$I = Ft \quad (16)$$

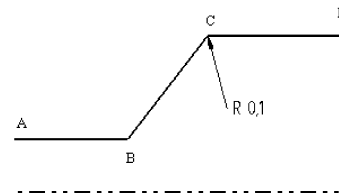


Fig. 16. Sharp edge treatment (grain).

### 3. Hyper-heuristics optimization approach

#### 3.1. Need of hyper-heuristic approach

The No Free Lunch Theorem proved that there is no one algorithm that could beat all other algorithms in all classes of problems. If an algorithm outperforms other algorithms on a specific class of problems, there must exist another class of problems on which this algorithm is worse than the others. Hence, a good way to raise the generality of heuristics is to apply different heuristics at different times of the search [7]. In this context, a generalized approach (termed hyper-heuristics) is proposed [12] which, broadly describes the process of using heuristics to choose heuristics to solve the problem [9,30].

Although there has been a momentous research done in the field of solid rocket motor design and optimization, but it is still unclear what kind of search method should be employed that is good enough to be applied on the vast range of problems. There have been instances of applying individual heuristics, hybrid heuristics, probabilistic methods and even gradient methods in rocket based vehicles design and optimization. Therefore, in current research effort we aim to move a step further and apply hyper-heuristic approach. Hyper-heuristic approach, presented in this research effort, selects optimizers of genetic algorithm, swarm intelligence and simulated annealing to perform simultaneous search.

The conceptual design of SRM involves optimization with design variables involving multiple disciplines. This results in increase of volume of the design space exponentially and makes solution space critically sensitive of various mission scenarios. The feasible design space of large problems is often non-convex and may contain multiple local optima. This can trap optimizers and prevent them from locating the best design. Heuristic optimization methods require significant parameter tuning of algorithms for the new problem or the new problem instance. Variation in design scenarios can lead to exhaustive search for the new problem instance. This discussion leads to adopt hyper-heuristic approach. The aim is to devise an algorithm for solving a problem that is independent of problem scenario, reasonably comprehensible, trustable in terms of quality and repeatability and with good behavior and

perform exceptional search for global optima and avoid local minima.

### 3.2. Working of proposed hyper-heuristic approach (HHA)

The choice of control function can be critical in setting an HHA. The bias of the control function can affect the performance both in solution quality and computational cost. Statistically, random sampling has advantages, as it produces unbiased estimates of the mean and the variance of the output variables. The choice of random function is attractive, from the perspective of increasing generality and avoiding bias of control function. The approach presented in this study uses a non-learning stochastic function applied to low-level meta-heuristics. The primary purpose is to avoid local minima and not selection of appropriate meta-heuristics. The purpose is not to reduce the computational time and selection of heuristic but to improve solution quality. The approach is simple, straightforward and easy to implement. The complexity of the inter-disciplinary problem demands quality of the solution to reduce the cost and time in life-cycle of product design phase. The proposed methodology attains the defined objective by providing diversity to population and altering search direction variations by injecting feasible solutions. This, however, may lead to additional computational time but at the same will serve as a tool to avoid local minima saving time in the longer run. Brief description of the low level meta-heuristics applied in this study is listed below.

Genetic algorithm uses a population of candidates to explore several areas of a solution space, simultaneously and adaptively. Ref. [16] developed genetic algorithms, which are capable of finding the global-optimal solution (or acutely near solutions) in complex, multidimensional search spaces. Details on GA can be found in Ref. [18]. GA applications have gained enormous popularity among aerospace professionals in the last decade [19,28]. This is due to the ease with which GA can be implemented and its exceptional ability to solve difficult complex problems more efficiently. The limitation of the GA is that it usually demands a large number of function evaluations [28].

Swarm intelligence is a new realm of research in that the PSO technique takes inspiration from social behavior of insects and animals. PSO technique models such social behavior as optimization algorithm, which guides a population of particles (the swarm) in different positions moving towards the most promising sector of the search space with different velocities. Each particle remembers its own best position found so far in the exploration and moves to the direction defined by its own best position and global best position, which is the best found so far by all particles. The position of each particle is updated in every iteration by adding the velocity vector to the position vector. Refs. [20,21] describe a complete chronicle of the development of PSO algorithm from just a motion simulator to an heuristic optimization technique.

Simulated annealing (SA) is a stochastic heuristic algorithm used to solve combinatorial optimization problems. SA was originally proposed by Metropolis [25] in the early 1950s as a model of the crystallization process. It was only in 1980s, that independent research, done by Refs. [8,23] noted similarities between physical process of annealing and some combinatorial optimization problems. They noted that there is a correlation between the different physical states of the matter and the solution space of an optimization problem. It was also observed that the objective function of an optimization problem corresponds with the free energy of the material. SA is well capable of working individually and in combination with other optimization methods in search of optimum results in multidisciplinary environment [29]. Fig. 17 presents the flow chart of hyper-heuristic approach. Pseudo-code of the proposed approach is given below.

#### Optimization routine

Initialize

- Set population size
- Set outer loop iteration
- Set inner loop iteration
- Set convergence criteria

**While** (convergence NOT achieved)

- Create public-board to store information
- Generate sub-population (random)
- Generate sub-iterations (random)

For  $i = 1$  to outer loop iteration

**OUTER LOOP**

For  $l = 1$  to sub-iteration

For  $j = 1$  to sub-population size

**Call** HEURISTICS(GA, PSO, SA)

**Evaluate Constraints**  
**Evaluate Fitness**  
**Store global best**  
**Store local best**

End

**CALL** OFF-SPRINGS FUNCTIONS

**Create new off-springs**  
**Send information to Public-board**

End

**INNER LOOP**

**CALL** POPULATION HANDLING

**Shuffle  $m\%$  of new population given to  $n$  optimizer**  
**Generate new sub-population (random)**  
**Generate new sub-iteration (random)**

**CALL** POPULATION DIVERSIFICATION

**IF** (outer loop iteration  $\leq \epsilon$ )  
Insert local best to sub-population (random)  
End

**IF** (outer loop iteration  $\geq \lambda$ )  
Insert global best to sub-population (random)  
End

End

**End**

**MAIN LOOP**

## 4. Experimental setup

### 4.1. Benchmark test functions

A comprehensive empirical analysis investigates the performance of hyper-heuristic algorithm. Table 1 summarizes 7 test functions used to evaluate the proposed algorithm. No. of variables, upper and lower bounds and objective function is also tabulated in Table 1. Below is the brief description of selected test functions.

- (1) De Jong function [11] is continuous, convex, uni-modal and one of the simplest benchmark tests.
- (2) The 2D six-hump camel back function [14] is a global optimization test function. There are six local minima and two global minima of this function.
- (3) The Ackley Problem [1] has several local minima but only one global minimum. It is a widely used multi-modal test function.
- (4) Schwefel's function [32] is deceptive in that the global minimum is geometrically distant, over the parameter space, from the next best local minima. The surface of this function comprises of a great number of peaks and valleys. Therefore, the



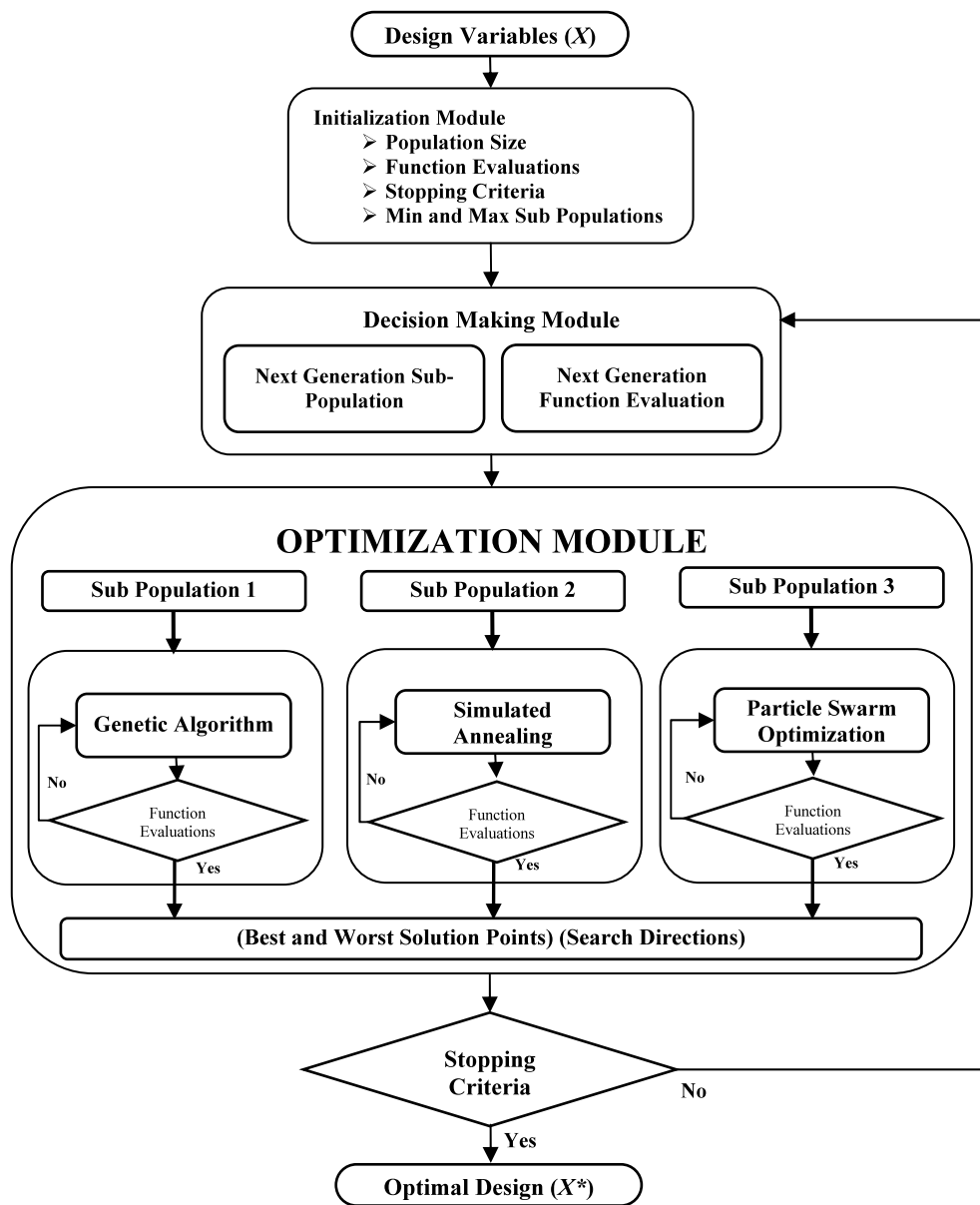


Fig. 17. Hyper-heuristic approach.

Table 1 Test functions.

Name of test function	Objective	No of variables (n)	[LB, UB]	Global optimum
De Jong (sphere)	$f(x) = \sum_{i=1}^n (x_i^2)$	30	[-100, 100]	0.0
Six-hump camel back	$f(x) = x_1^2(4 - 2.1x_1^2 + 1/3x_1^4) + x_1x_2 + 4x_2^4 - 4x_2^2$	02	[-3, 3]	-1.031628
Ackley	$f(x) = 20 + e - 20e^{(-0.2\sqrt{1/n \sum_{i=0}^n x_i^2})} - e^{(\frac{1}{n} \sum_{i=0}^n \cos(2\pi x_i))}$	10	[-30, 30]	0.0
Schwefel	$f(x) = \sum_{i=0}^n -x_i \sin \sqrt{ x_i }$	02	[-500, 500]	-418.9829n
Rosenbrock	$f(x) = \sum_{i=1}^{n-1} (1 - x_i^2) + 100(x_{i+1} - x_i^2)^2$	20	[-30, 30]	0.0
Rastrigin	$f(x) = \sum_{i=1}^n (x_i^2 - 10 \cos(2\pi \cdot x_i) + 10)$	20	[-5.12, 5.12]	0.0
Griewank	$f(x) = \frac{1}{4000} \sum_{i=0}^n x_i^2 - \prod_{i=0}^n \cos(\frac{x_i}{\sqrt{i}} + 1)$	10	[-600, 600]	0.0

search algorithms are potentially vulnerable to convergence in the wrong direction. This problem has many local minima and requires a large number of function evaluations to reach at the global minimum.

- (5) Rosenbrock function [13] is a classic optimization problem, also known as banana function or the second function of De Jong. The global minimum is inside a long, narrow, parabolic-shaped flat valley. To locate the valley is trivial, however, con-

vergence to the global optimum is difficult and hence it has been frequently used to assess the performance of optimization algorithms.

- (6) Rastrigin's function [37] is often used to evaluate global optimizers. This function is a remarkably difficult problem due to its large search space and the large number of local minima. The function is highly multi-modal, and the locations of the minima are regularly distributed.

**Table 2**  
Results of test functions.

S. No.	Test function	Success rate	Mean value	Standard deviation	Average function evaluations
1	De Jong (sphere)	100%	1.99E-05	5.49015E-05	2953
2	Six-hump camel back	99%	-1.0316	2.1664E-007	7454
3	Ackley	98%	7.89E-06	0.000466	42 208
4	Schwefel	99%	-4.189E+02	3.39E-10	7551
5	Rosenbrock	100%	1.18E-06	4.88E-06	11 912
6	Rastrigin	98%	7.89E-06	1.4E-05	28 728
7	Griewank	98%	2.21E-05	5.34E-05	32 028

(7) The Griewank function, first introduced in [17], has been widely employed as a test function for global optimization algorithms. Its number of minima grows exponentially as its number of dimensions increases. The fast increasing number of local minima suggests that the global minimum becomes extremely difficult to detect.

#### 4.2. Results of test functions

In experiments, population size is set at 100, and the all the test functions are executed for 100 times with the same algorithm parameter settings. In order to investigate the quality of the algorithm, a fair measure must be selected. The simulation is considered successful if the solution is less than  $|4e-4|$  of the true global minimum. Table 2 reveals the results obtained.

Results reveal that hyper-heuristic approach performed magnificently for solving these classical test functions. On the robustness of algorithms, hyper-heuristic approach is significantly capable of finding the global optimum with superb success rate on all the test functions. HHA proves to be a highly stable algorithm, capable of obtaining consistent results in terms of accuracy and robustness.

### 5. Solid rocket motor test case

SRM sub-systems are mass or volume (or both) constrained depending upon the specific application. Specific impulse and initial to burn-out mass ratio affects the burn-out vehicle velocity as a natural log function. This drives the SRM design towards lighter weight components, and high energy propellants. The fundamental drivers of SRM design are maximization of specific impulse and minimization of inert mass. Design practice dictates meeting these objectives while satisfying mission constraints. Selection of design variables can be critical, present study includes eight variables that are geometrical and ballistic in nature. SRM for this study uses a steel casing with conical nozzle, requiring a minimum total impulse of 39 500 under specified constraints.

#### 5.1. Design objective

There can be different objective functions for SRM optimization problems. Traditionally minimum gross mass have been sought as it is a strong driver on performance. For the present research effort, design objective is to minimize the gross mass of motor that indeed would cater for a minimum inert mass along with maximum specific impulse. Mathematical description of design objective is as under:

$$\min M_{gross}(X) \quad (17)$$

Gross mass is given by

$$M_{gross} = m_p + M_C + M_i + M_N \quad (18)$$

whereas design variables  $X$  are given in Eq. (20);

$$X = f(\psi, D, p_c, \varepsilon, t, \alpha, \beta, L) \quad (19)$$

Details of the objective function calculations are summarized as follows:

1. Chamber pressure, nozzle area ratio and propellant characteristics come from the decision variables.
2. Determine thrust coefficient using Eq. (15).
3. Determine specific impulse from

$$I_{sp} = C_F c^* \eta_{isp} \quad (20)$$

4. Determine propellant mass by using following equation:

$$m_p = \frac{I}{I_{sp} g} \quad (21)$$

5. Determine propellant and casing volume from

$$V_p = \frac{m_p}{\rho_p} \quad (22)$$

$$V_{case} = \frac{m_p}{\rho_p \eta_{vol}} \quad (23)$$

6. Determine nozzle throat area, throat diameter and exit diameter from following equations:

$$A_t = \frac{m_p g I_{sp}}{C_F p_c t} \quad (24)$$

$$d_t = \sqrt{\frac{4A_t}{\pi}} \quad (25)$$

$$d_e = \sqrt{\varepsilon} d_t \quad (26)$$

7. Determine casing thickness through Eq. (1).
8. Determine average thrust by through Eq. (14).
9. Determine insulation thickness in chamber and nozzle using Eqs. (2)–(11).
10. Determine casing mass and available volume using model shown in Fig. 3.
11. Determine insulation mass using model shown in Fig. 4.
12. Determine nozzle profile using model shown in Fig. 6.
13. Determine mass of nozzle components using models shown in Figs. 7–12.
14. Construct Finocyl grain geometry using models shown in Figs. 13–16. Perform grain geometric regression. Eq. (12) determines burning area ~ web relation.
15. Perform internal ballistics and determine pressure and thrust time histories.

Fig. 18 presents a flow chart for the objective function calculation.

#### 5.2. Design variables

Table 3 lists the system design variables for entire SRM each stage with respective discipline. There are total of 8 design variables that govern the integrated design and optimization problem of SRM.

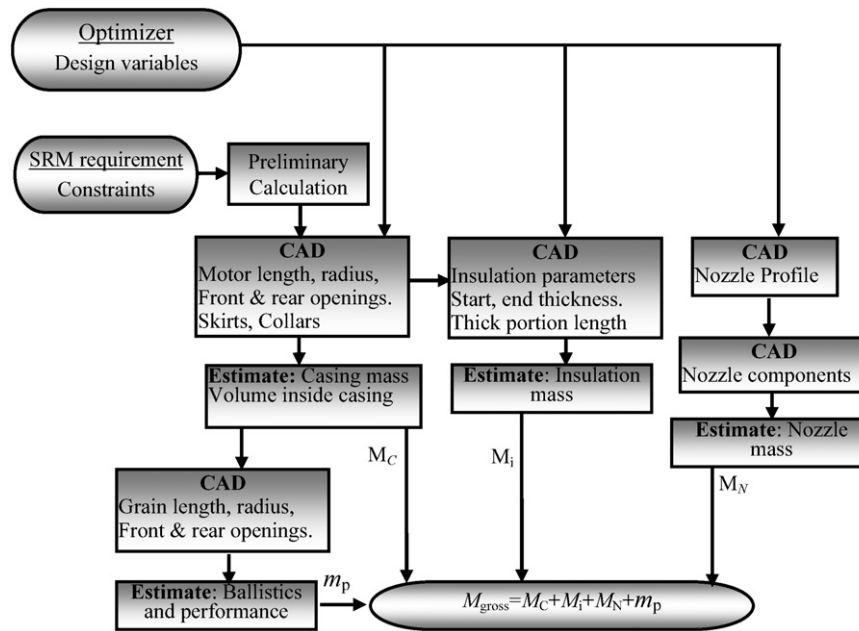


Fig. 18. Flowchart of optimization process.

5.3. Design constraints

SRM working envelope, manufacturing and propellant type impose several stringent constraints on design. Targeted design of SRM is for use as 1st stage or booster stages therefore  $L/D$  ratio, diameter, chamber pressure, area ratio, burn time, convergent and divergent angles, length, exit diameter, maximum thrust and total impulse are constrained for targeted use. Constraints are formulated as under:

$$C_i \geq 0, \quad i = 1, 2, \dots, 11$$

where  $C$  is given as:

$$C_1: \quad 4.5 \leq \lambda \leq 7$$

$$C_2: \quad 1200 \leq D \leq 1400$$

$$C_3: \quad 50 \leq p_c \leq 80$$

$$C_4: \quad 10 \leq \varepsilon \leq 20$$

$$C_5: \quad 60 \leq t \leq 80$$

$$C_6: \quad 50 \leq \alpha \leq 60$$

$$C_7: \quad 16 \leq \beta \leq 20$$

$$C_8: \quad L \leq 9500$$

$$C_9: \quad d_e \leq 900$$

$$C_{10}: \quad F \geq 570$$

$$C_{11}: \quad I \geq 39500 \tag{27}$$

6. Results and discussion

Design and optimization using hyper-heuristic approach is successfully implemented for complex design problem of solid rocket motor under stringent mission objectives and performance constraints. Proposed hyper-heuristic proved to be remarkably effective in terms of exploring the design space and fulfilling design objectives.

Table 4 contains optimal values for all the design variables. Optimized design variables of design space of SRM lie between

Table 3 System design variables.

Design variable	Discipline	Symbol	Units
Length to diameter ratio of grain	Envelope	$\psi$	Ratio
Chamber diameter	Chamber	$D$	mm
Chamber pressure	Grain-ballistic	$p_c$	bar
Nozzle area ratio	Nozzle-ballistic	$\varepsilon$	-
Motor operating time	Grain-ballistic	$t$	s
Convergent angle	Nozzle	$\alpha$	deg
Divergent angle	Nozzle	$\beta$	deg
Length of motor	Envelope	$L$	mm

Table 4 Optimum design variables.

Design variable	Symbol	Units	Optimum value
Length to diameter ratio of grain	$\lambda$	Ratio	6.11
Chamber diameter	$D$	mm	1326.3
Chamber pressure	$p_c$	bar	75.3
Nozzle area ratio	$\varepsilon$	-	14.16
Motor operating time	$t$	s	69.48
Convergent angle	$\alpha$	deg	57.4
Divergent angle	$\beta$	deg	18.4
Length of motor	$L$	mm	9454.5
Average thrust	$F$	kN	571.59

Table 5 SRM sub-system mass breakdown.

Design variable	Symbol	Units	Optimum value
Propellant mass	$M_p$	kg	14666
Casing mass	$M_c$	kg	1650.7
Insulation + liner mass	$M_i$	kg	344.7
Nozzle mass	$M_n$	kg	251.2
Total inert	$I_m$	kg	2246.6
Gross mass	$G_M$	kg	16912.6

their upper and lower bounds. Results reveal that SRM is capable of completing the specified mission through hyper-heuristic based design and optimization approach. Table 5 lists the mass breakdown of SRM components of optimized configuration. Finocyl grain configuration is adopted for present case; it can provide a large

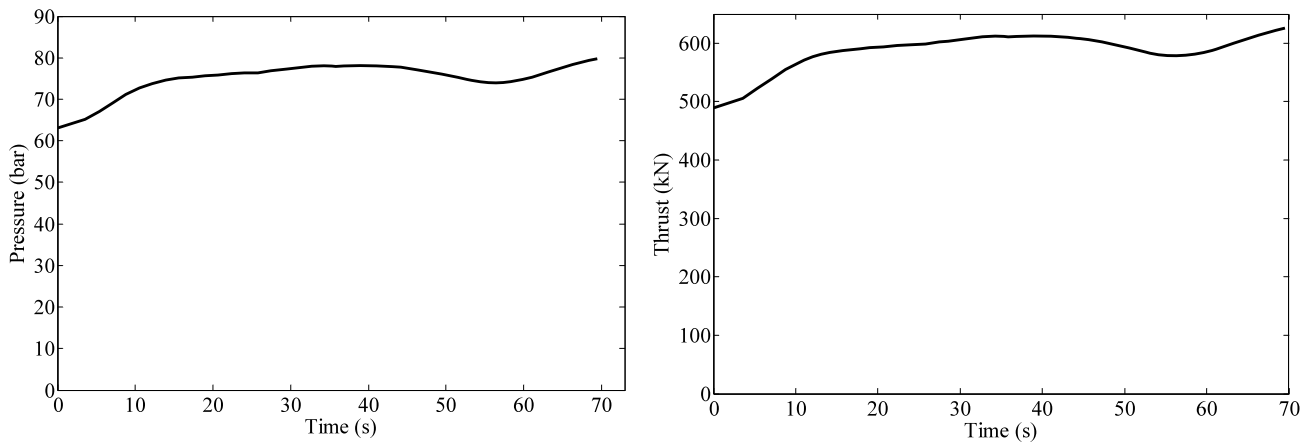


Fig. 19. Ballistic performance of optimal SRM configuration.

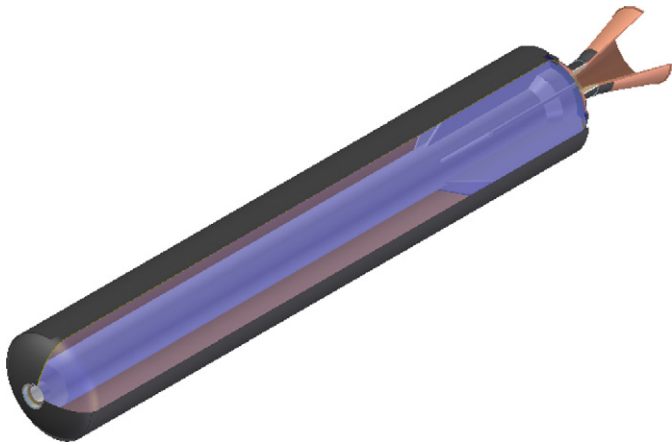


Fig. 20. Optimal SRM assembly.

thrust at start due to high initial burning area that can be provided by fins. The constraint on initial thrust makes Finocyl grain configuration to be a better choice. Finocyl grain configuration design proved the viability of the optimized SRM. Thrust time trace agrees fairly well with desired impulse and ballistic parameter constraints (Fig. 19). Fig. 20 presents optimal SRM assembly. Table 6

summarizes SRM sub-systems details of the optimal configuration. For the test case, minimum gross mass of 16912.6 kg is achieved with all the stringent constraints being satisfied. It can be concluded that the proposed integrated modeling and optimization module provides a proficient platform in facilitating design analysis and optimization of solid rocket motor.

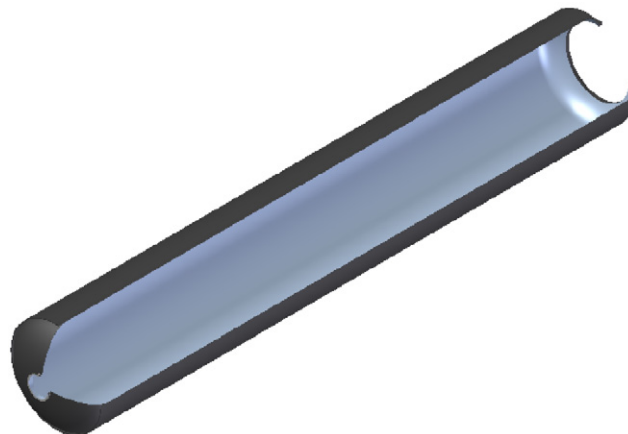
## 7. Conclusion

The present research effort implements an automated approach for the design and optimization of SRM. CAD software is integrated with optimization module. CAD modeling overcomes the limitation posed by analytical expression thus increased model fidelity. CAD model allows different sub-systems to be modeled separately that not only prevents feature creation failures but also allows ease in modification of the model. Grain design is vital component of SRM design. This research effort also included grain regression simulation.

Hyper-heuristic approach eliminates the necessity of suitable initial guess and parameter tuning. The approach significantly increases the ability to search optimal solutions without adequate tuning of the algorithm for different problem scenarios. This methodology can handle optimization problem in the area of solid rocket motor system design, where the optimization of several

**Table 6**  
SRM sub-system details (all units in mm).

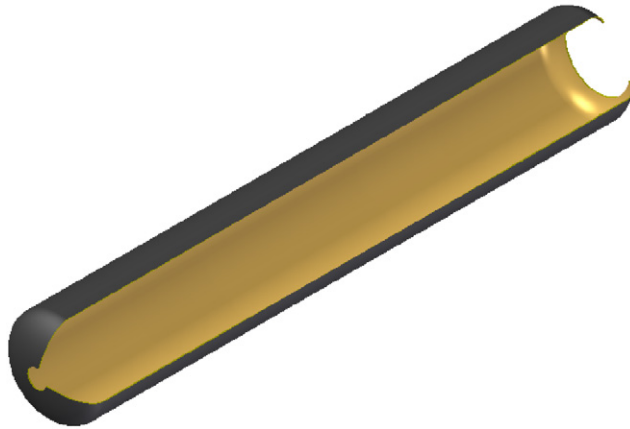
Casing dimension	
Chamber length	= 8105.6
Chamber radius	= 663.15
Chamber thickness	= 5.76
Front end opening	= 132.6
Rear end opening	= 464.2
Front collar width	= 23.04
Front collar thickness	= 17.2
Front skirt thickness	= 11.5
Front skirt length	= 119.1
Rear end thickness	= 11.5
Rear end collar thickness	= 33.5
Rear end collar width	= 33.5
Rear end skirt length	= 119.1
Front end skirt width	= 11.5



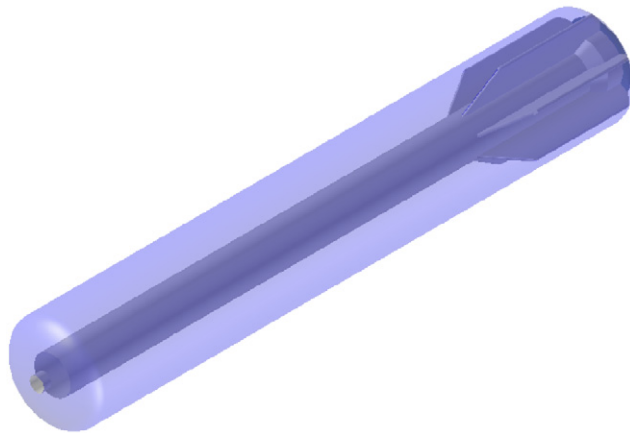
(continued on next page)

**Table 6** (continued)**Insulation dimension**

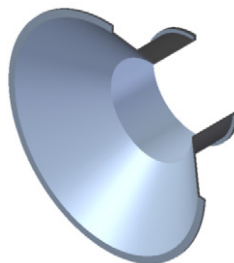
Length,  $L1 = L2 = 2652.6$   
 Nominal thickness = 2.24  
 Front start thickness = 18.6  
 Front end thickness = 14.5  
 Rear start thickness = 18.6

**Grain dimension**

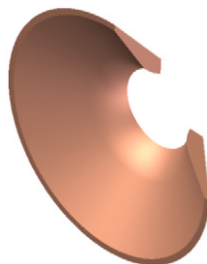
Front web = 115  
 Front end opening = 133  
 Front cone = 110  
 Grain bore = 260  
 Rear cone = 167.3  
 Rear cylinder length = 210  
 Rear cylinder diameter = 350  
 No of fins = 6  
 Fin length = 1400  
 Fin radius = 84  
 Fin angle = 32 deg  
 Fin height = 600  
 Fin width = 43.4

**Nozzle convergent metallic section**

Convergent front collar thickness = 8.9  
 Convergent front collar width = 29.9  
 Convergent thickness = 7.48  
 Convergent rear collar thickness = 14.9  
 Convergent rear collar width = 22.5

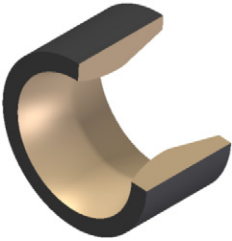
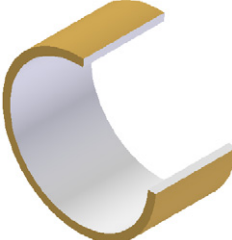
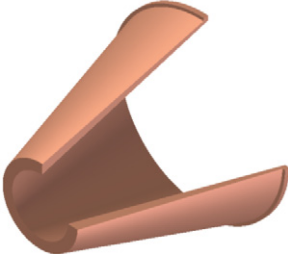

**Nozzle convergent section**

Convergent insulation start thickness = 15.9  
 Convergent insulation end thickness = 60.4  
 Convergent angle = 57.4°



(continued on next page)

Table 6 (continued)

Nozzle throat section Throat maximum thickness = 65 Throat length = 225	
Nozzle throat insulation Throat insulation length = 225 Throat insulation thickness = 20.4	
Nozzle divergent section Divergent start thickness, 52.3 Divergent end thickness, 17.6 Divergent angle = 18.4°	
Nozzle divergent metallic support Divergent support collar width = 22.5 Divergent support collar thickness = 7.5 Divergent support length = 125 Divergent support tapered length = 62.5 Tapered end thickness = 3.74	

interdisciplinary design variables and considering conflicting constraints are present.

## References

- [1] D.H. Ackley, A Connectionist Machine for Genetic Hill-Climbing, Kluwer, Boston, 1987.
- [2] M. Anderson, J. Burkhalter, Multi-disciplinary intelligent systems approach to solid rocket motor design, Part I: single and dual goal optimization, AIAA 2001-3599.
- [3] M. Anderson, J. Burkhalter, Multi-disciplinary intelligent systems approach to solid rocket motor design, Part II: single and dual goal optimization, AIAA 2001-3600.
- [4] Marcel Barrere, et al., Rocket Propulsion, Elsevier Publishing Company, Amsterdam, 1960.
- [5] J.S. Billheimer, Optimization and design simulation in solid rocket design, AIAA 68-488.
- [6] James Brill Clegern, Computer aided solid rocket motor conceptual design and optimization, AIAA 94-0012.
- [7] E. Burke, E. Hart, G. Kendall, J. Newall, P. Ross, S. Schulenburg, Hyper-heuristics: an emerging direction in modern search technology, in: F. Glover, G. Kochenberger (Eds.), Handbook of Meta-Heuristics, Kluwer, 2003, pp. 457–474.
- [8] O. Cerny, Thermodynamical approach to the travelling salesman problem: an efficient simulation algorithm, Journal of Optimal Theory and Applications 45 (1) (1985) 41–51.
- [9] P. Cowling, E. Soubeiga, Neighborhood structures for personnel scheduling: a summit meeting scheduling problem, in: 3rd International Conference on the Practice and Theory of Automated Timetabling, Germany, Aug. 2000.
- [10] A. Davenas, Solid Rocket Propulsion Technology, Elsevier Science & Technology, 1993.
- [11] K. De Jong, An analysis of the behavior of a class of genetic adaptive systems, PhD thesis, University of Michigan, 1975.
- [12] J. Denzinger, M. Fuchs, M. Fuchs, High performance ATP systems by combining several AI methods, in: 15th International Joint Conference on Artificial Intelligence (IJCAI '97), 1997, pp. 102–107.
- [13] L.C.W. Dixon, D.J. Mills, Effect of rounding errors on the variable metric method, Journal of Optimization Theory and Applications 80 (1) (1994) 175–179.
- [14] L.C.W. Dixon, G.P. Szego, The optimization problem: an introduction, in: L.C.W. Dixon, G.P. Szego (Eds.), Towards Global Optimization II, North Holland, New York, 1978.
- [15] Z. Fang, G. Guo, Optimization design of the solid rocket motor, Journal of Aerospace Power 5 (Apr. 1990) 176–178.
- [16] D. Goldberg, Genetic Algorithms in Search, Optimization and Machine Learning, 1st ed., Addison-Wesley Longman, Reading, MA, 1989.

- [17] A.O. Griewank, Generalized descent for global optimization, *Journal of Optimization Theory and Applications* 34 (1) (1981) 11–39.
- [18] J.H. Holland, *Adaptation in Natural and Artificial Systems: An Introductory Analysis with Applications to Biology, Control, and Artificial Intelligence*, MIT Press, Cambridge, MA, 1992.
- [19] A. Kamran, L. Guozhu, Design and optimization of 3D radial slot grain configuration, *Chinese Journal of Aeronautics* 23 (4) (2010) 409–414.
- [20] J. Kennedy, R.C. Eberhart, *Swarm Intelligence*, Morgan Kaufmann, San Mateo, CA, 2001.
- [21] J. Kennedy, R. Eberhart, Particle swarm optimization, in: *Proceedings of the IEEE International Conference on Neural Networks*, Perth, Australia, 1995, pp. 1942–1945.
- [22] N. Khurram, L. Guozhu, Z. Qasim, A hybrid optimization approach for SMR Finocyl grain design, *Chinese Journal of Aeronautics* 21 (6) (Dec. 2008) 481–487.
- [23] S. Kirkpatrick, C.D. Gelatt, M. Vecchi, Optimization by simulated annealing, *Journal of Science* 220 (4598) (1983) 498–516.
- [24] W.J. Mc Cain, A variable selection heuristic for solid rocket motor, PhD dissertation, University of Alabama in Huntsville, Number 9324488, 1993.
- [25] N. Metropolis, A.W. Rosenbluth, M.N. Rosenbluth, A.H. Teller, E. Teller, Equations of state calculations by fast computing machines, *Journal of Chemical Physics* 21 (6) (1953) 1087–1092.
- [26] J.R. Olds, The suitability of selected multidisciplinary design techniques to conceptual aerospace vehicle design, *AIAA* 92-4791.
- [27] J. Peterson, J. Garfield, The automated design of multi-stage solid rocket vehicles, *AIAA* 76-744.
- [28] A.F. Rafique, H. LinShu, A. Kamran, Q. Zeeshan, Multidisciplinary design of air launched satellite launch vehicle: performance comparison of heuristic optimization methods, *Acta Astronautica* 67 (7–8) (2010) 826–844, doi:10.1016/j.actaastro.2010.05.016.
- [29] A.F. Rafique, H. LinShu, Q. Zeeshan, A. Kamran, K. Nisar, Multidisciplinary design and optimization of an air launched satellite launch vehicle using a hybrid heuristic search algorithm, *Journal of Engineering Optimization* 43 (3) (2011) 305–328, doi:10.1080/0305215X.2010.489608.
- [30] P. Ross, Hyper-heuristics, in: E.K. Burke, G. Kendall (Eds.), *Search Methodologies: Introductory Tutorials in Optimization and Decision Support Techniques*, Springer, 2005, pp. 529–556 (Chapter 17).
- [31] Daniel M. Schumacher, A system level model for preliminary design of a space propulsion solid rocket motor, PhD dissertation, University of Alabama in Huntsville, Number 3181448, 2005.
- [32] H.P. Schwefel, *Numerical Optimization of Computer Models*, Wiley & Sons, Chichester, 1981.
- [33] R.H. Sforzini, An automated approach to design of solid rockets utilizing a special internal ballistic model, *AIAA* 80-1135.
- [34] J. Sobieszcanski-Sobieski, R.T. Haftka, Multidisciplinary aerospace design optimization: survey of recent developments, *Journal of Structural Optimization* 14 (1) (1997) 1–23.
- [35] P. Sutton, B. Oscar, *Rocket Propulsion Elements*, 7th ed., Wiley-Interscience, 2001.
- [36] V. Swaminathan, N.S. Madhavan, A direct random search technique for the optimization of propellant systems, *The Journal of the Aeronautical Society of India* 32 (1980).
- [37] A. Törn, A. Ziliinskas, *Global Optimization, Lecture Notes in Computer Science*, vol. 350, Springer-Verlag, Berlin, 1989.
- [38] A. Truchot, Overall optimization of solid rocket motors, *AIAA* 89-16916.
- [39] T. Walsh, R. Wartburg, Ballistic missile sizing and optimizing, *AIAA* 78-1019.
- [40] Guanglin Wang, E. Cai, *The Design of Solid Rocket Motor*, Northwestern Polytechnical University Press, 1994.
- [41] D.H. Wolpert, W.G. Macready, No free lunch theorems for optimization, *IEEE Transactions on Evolutionary Computation* 1 (1) (1997) 67–82.